




 Cite this: *RSC Adv.*, 2021, 11, 6958

# Current advances in nanomaterials affecting morphology, structure, and function of erythrocytes

 Yaxian Tian,<sup>ab</sup> Zhaoju Tian,<sup>b</sup> Yanrong Dong,<sup>a</sup> Xiaohui Wang <sup>\*a</sup>  
 and Linsheng Zhan <sup>\*a</sup>

In recent decades, nanomaterials have been widely used in the field of biomedicine due to their unique physical and chemical properties, and have shown good prospects for *in vitro* diagnosis, drug delivery, and imaging. With regard to transporting nanoparticles (NPs) to target tissues or organs in the body intravenously or otherwise, blood is the first tissue that NPs come into contact with and is also considered an important gateway for targeted transport. Erythrocytes are the most numerous cells in the blood, but previous studies based on interactions between erythrocytes and NPs mostly focused on the use of erythrocytes as drug carriers for nanomedicine which were chemically bound or physically adsorbed by NPs, so little is known about the effects of nanoparticles on the morphology, structure, function, and circulation time of erythrocytes in the body. Herein, this review focuses on the mechanisms by which nanoparticles affect the structure and function of erythrocyte membranes, involving the hemocompatibility of NPs, the way that NPs interact with erythrocyte membranes, effects of NPs on erythrocyte surface membrane proteins and their structural morphology and the effect of NPs on erythrocyte lifespan and function. The detailed analysis in this review is expected to shed light on the more advanced biocompatibility of nanomaterials and pave the way for the development of new nanodrugs.

 Received 1st December 2020  
 Accepted 27th January 2021

DOI: 10.1039/d0ra10124a

[rsc.li/rsc-advances](http://rsc.li/rsc-advances)

## 1 Introduction

Along with the rapid development of nanotechnology, nanomaterials are finding a wide range of applications in biomedical fields such as biosensors, bioimaging, drug/gene delivery, and oncology therapy. NPs can be classified into different species, including carbon-based NPs, metal NPs, ceramic NPs, and polymer NPs<sup>1</sup> based on their compositions. With the increasing complexity of their unique physicochemical properties, implant sites, and potential applications in nanomedicine, the biosafety of nanomaterials is becoming a major concern.<sup>2</sup> NPs enter the body circulation mostly *via* the intravenous drug delivery route to exert their function, while their particle size is small and can be easily distributed throughout the body and cross the biological barrier so that the interactions of NPs with blood components are inevitable and potentially dangerous.<sup>3</sup>

Erythrocytes are not only the most abundant cells in the circulatory system, but also the first cell type that NPs meet with after entering the blood circulation through intravenous injection. Erythrocytes have a simple structure without nuclei or

mitochondria, the shape, stability, and deformability of which mainly depends on the cytoskeleton. The most important biological function of erythrocytes is the oxygen-carrying capacity, which sustains the normal life activities of organisms by transporting oxygen and carbon dioxide. So far, researches on the relationship between nanomaterials and erythrocytes have focused on the feasibility of using erythrocytes as a bionic drug carrier to prolong the drug half-life *in vivo* or target the lesion site. On the whole, for the effort of quality control in construction of erythrocytes camouflaged NPs, such as the measurement of hemolysis, PS externalization, band 3 and so on, the basically properties of plasma membrane of red blood cells are maintained for these NPs to some extent, consequently it is reasonable to look forward to the good hemocompatibility of them. Thus these researches are beyond the scope of this review. This paper is exclusively concerned with nanomaterials that have not undergone chemical bonding or physical adsorption with erythrocytes or their outer membrane for the main purpose of exploring their possible side effects on erythrocytes when in close contact with blood circulation. Herein, as for common carbon-based NPs (fullerenes and graphene), metal NPs (gold nanoparticles, silver nanoparticles, metal oxides), and some silicon-based NPs, we will highlight their effects on erythrocyte membrane proteins, membrane enzymes, and membrane surface molecules, as well as erythrocyte

<sup>a</sup>Institute of Health Service and Transfusion Medicine, Beijing 100850, People's Republic of China. E-mail: lovechina1980@163.com; lszhan91@yahoo.com

<sup>b</sup>School of Public Health, Shandong First Medical University, Shandong Academy of Medical Sciences, Taian, Shandong 271016, China



lifespan and function. It is hoped that the analysis in this review would contribute to the design of nanodrug screening and to the blood compatibility of nanodrugs.

## 2 Blood compatibility of NPs

### 2.1 Hemolytic properties of NPs

Erythrocytes are the most abundant blood cells in blood, and also one of the first active components that nanomedicine comes into contact with when administered intravenously. Since many studies have focused on the hemolysis properties of NPs, few have attempted to explore the underlying mechanism. Besides such physicochemical properties of NPs as surface charge, particle size and oxygen content, the generation of reactive oxygen, lipid peroxidation, and other external factors may also have strong impacts on hemolysis activity.

Since 2011, a large number of researchers have devoted themselves to studies on blood compatibility of graphene oxide (GO), with special attention to their biological distribution, histopathological analysis, and effects on the structure and function of important blood components.<sup>4–6</sup> Hsuan *et al.* prepared GO and graphene sheets (GS) with various sizes and different extents of exfoliation and oxygen contents using a simple aqueous and hydrazine-free hydrothermal route combined with ultrasound treatment, namely GO, bGO, pGO-5, pGO-30, GS (which obtained from pGO-5 by hydrothermal treatment in D. I. water for 20 h). The hemolytic properties were systematically evaluated. Results showed that both GO and GS disrupted erythrocyte membranes in a concentration-dependent manner, and both particle size and surface charge or oxygen content could have a significant influence on blood

compatibility of NPs. Subsequently, they coated pGO-30 which had the greatest hemolytic activity with the biocompatible polymer chitosan to obtain expected pGO-30/chitosan. Compared to pGO-30, no significant hemolysis was observed in pGO-30/chitosan, suggesting that the hemolysis of pGO-30 might have been caused by the altered electrostatic interaction between oxygen groups and erythrocytes, or due to aggregation states of NPs which affected the cell-contactable surface area.<sup>4</sup> Liu and colleagues investigated the hemolytic effect of C<sub>2</sub>N, a novel 2D nanomaterial, on erythrocytes, and found that compared to highly hemolytic reductive graphene oxide (rGO) nanosheets, erythrocytes treated by C<sub>2</sub>N had a rather low hemolysis rate ( $\approx 1.21 \pm 0.13\%$ ) even at a high concentration of 200  $\mu\text{g mL}^{-1}$ . This might be due to the fact that POPC membrane polarized lipid head groups and water molecules exhibited significant Coulomb force of attraction to both negative-charged pores and positive-charged benzene rings of C<sub>2</sub>N nanosheets (Fig. 1d). Thus, C<sub>2</sub>N tends to be adsorbed flatly onto the erythrocyte membrane, and the resistance created by this electrostatic interaction makes it difficult to penetrate the cell membrane and induce hemolysis (Fig. 1a and c). Low hemolysis demonstrates superior compatibility of C<sub>2</sub>N with human erythrocytes.<sup>7</sup> The hemolytic properties of NPs can also be determined by their geometry, surface characteristics, and chemical composition. In addition to their intrinsic properties, NPs are also influenced by a variety of external factors, including the type of culture medium, erythrocyte species, concentration, storage duration, animal health status, centrifugation rate, exposure time, and incubation temperature.<sup>8</sup> These studies have offered evidence that in the case of GO-related NPs, the high extent of exfoliation of the material, the

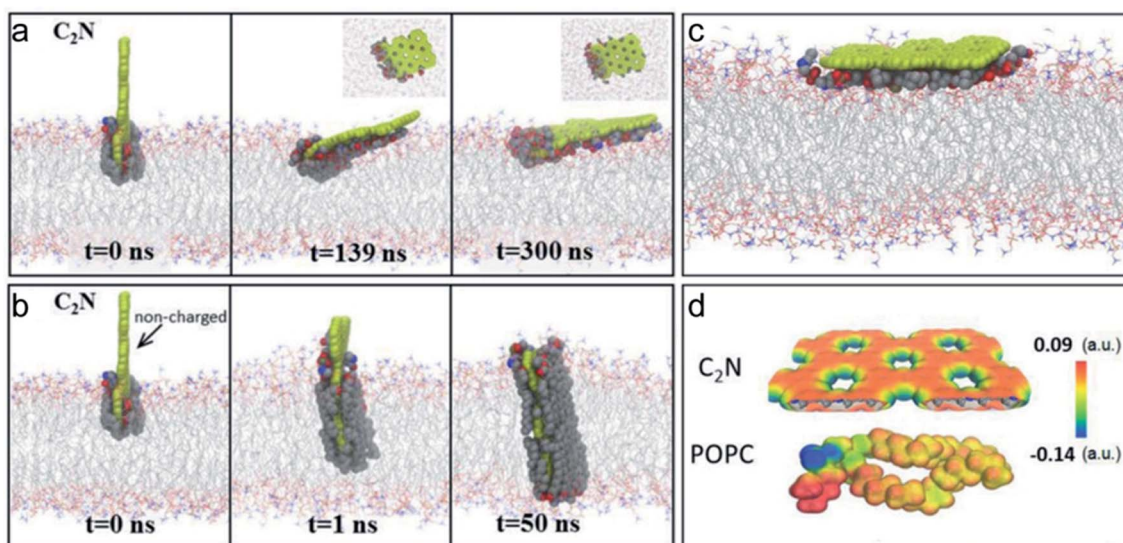


Fig. 1 (a and b) MD simulations show the representative trajectories of C<sub>2</sub>N and non-charged C<sub>2</sub>N on POPC membranes. C<sub>2</sub>N prefers to be adsorbed flatly to the erythrocyte membrane, while non-charged C<sub>2</sub>N is inserted into the lipid membrane. (c) The final combine information of C<sub>2</sub>N binding with POPC. (d) Electrostatic potentials of the C<sub>2</sub>N sheet and a single lipid molecule. Extracted atoms in membranes are shown by vdW spheres (red, O; blue, N; gray, C), the pore edges are negatively charged and benzene rings of the C<sub>2</sub>N nanosheets are positively charged. Notes: copyright obtained from ref. 7: (L. Liu, S. Zhang, L. Zhao, Z. Gu, G. Duan, B. Zhou, Z. Yang and R. Zhou, *Small*, 2018, **14**, 1803509.). Figure has been reproduced from ref. 7 with permission from the John Wiley and Sons, copyright 2021.





Table 1 Interactions of various nanoparticles with red blood cell membranes

| Nanoparticles                          | Interaction with membrane                                 |                  |           |                  |   |   |                           | Cytoskeletal proteins                        |   |   |
|--|---|------------------|-----------|------------------|---|---|---------------------------|--|---|---|
|  | Hemolytic properties                                      | Potassium efflux | LDH       | Membrane enzymes | Interaction modes   | Erythrocyte morphology  | Membrane permeability     |  | Membrane fluidity   | Membrane deformability                        |
| Carbon-based nanoparticles             | Prevent hemolysis and potassium efflux                    | No effect        | Increase  | Decrease         | Surface or insert   | Concentration dependence  | Increase ion permeability | Increase                                     | Decrease  | Possibility interaction Mild and biofriendly* |
| Metal nanoparticles                    | Fullerene related NPs <sup>1,12,25,34,38,39,45</sup>      | Hemolytic        |           |                  | Surface or insert   |   |                           |  |   |   |
|  | Graphene related NPs <sup>4,5,7,8,35,36,44</sup>          | Hemolytic        |           |                  | Surface or insert   |   |                           |  |   |   |
|  | Carbon nanotubes <sup>9,10,46</sup>                       | Hemolytic        |           |                  | Loose and stronger *  |   |                           |  |   |   |
|  | Gold related NPs <sup>29,49,66,80,81</sup>                | Hemolytic        |           |                  | Surface or enter  | Spherocytes and echinocytes   |                           |  | Decrease*   |   |
|  | Silver related NPs <sup>19,51,66-69,73,82</sup>           | Hemolytic        |           |                  | Enter   | Tiny depressions, echinocytes   |                           |  | Decrease  |   |
| Silica-based nanoparticles             | Titanium dioxide (TiO <sub>2</sub> ) <sup>31,75</sup>     | Hemolytic        |           |                  | Attach along or insert  | Spherocytes and echinocytes   | No effect                 |  |   |   |
|  | Fe <sub>3</sub> O <sub>4</sub> magnetic NPs <sup>63</sup> | Hemolytic        |           |                  | Aggregate, and adhere   | Eryptosis   |                           |  | Decrease  |   |
|  | Silica <sup>12-14,50,78,83-85</sup>                       | Hemolytic        |           |                  | Attach to the surface   | Echinocytes   |                           |  | Decrease  |   |
| Instrumentation techniques and methods | Photometry  | Flame photometer | Assay kit | Assay kit        | Optical microscopy, AFM, TEM, SEM, confocal fluorescence microscopy | Flow cytometry, optical microscopy, AFM, TEM, SEM, confocal fluorescence microscopy | Photometry                | Fluorescent probe (DPH/TMA-DPH/ANS/PDA), ESR | Laser-diffraction ektacytometer (LBY-BX), microfluidic ektacytometer, automatic blood rheometer | SDS-PAGE, western blot                        |

small particle size, and the increased concentration within a certain range all play positive roles in the hemolytic activity of NPs. GS has lower hemolytic activity due to the low oxygen content and fewer reactive oxygen groups accessible to erythrocytes, while their precursor material, graphene, has a lower surface area and greater hydrophobicity, therefore leading to weaker hemolytic properties. Due to its periodically distributed negative/positive potentials from the head groups of lipid molecules, C<sub>2</sub>N sheet showed unique electrostatic properties, and caused less damage to erythrocytes. Meanwhile, the incubation conditions also make much difference to the hemolysis property of GO, so there is the need to try to find the best incubation conditions during the experiment (Tables 1 and 2).

As for carbon nanotubes, optical absorption spectra confirmed that high concentrations of multi-walled carbon nanotubes (MWCNT, 50 μg mL<sup>-1</sup>) may form hydrated clusters that localize to the surface of erythrocyte, altering the structural organization of membrane integrins and accelerating hemolysis.<sup>9</sup> Single-walled carbon nanotubes (SWNTs) were demonstrated to enter into erythrocytes by the way of “membrane encapsulation” or “endocytosis”, and experimental results showed that bundled SWNTs could cause cell–cell fusion and had higher hemolytic activity than individual SWNTs alone.<sup>10</sup>

In addition to the toxic effects on erythrocytes, NPs have also been found to be able to protect erythrocytes somehow. Jacek Grebowski *et al.* irradiated human erythrocytes with 6 MeV high-energy electrons with 150 μg mL<sup>-1</sup> of polyhydroxylated fullerene C<sub>60</sub>(fullerenol C<sub>60</sub>(OH)<sub>36</sub>), and found that the presence of fullerenol C<sub>60</sub>(OH)<sub>36</sub> protected erythrocytes from hemolysis induced by high-energy electron irradiation, and the protective effect became much stronger with irradiation intensity and irradiation time. This protective effect was largely dependent on its ability to scavenge ROS. Meanwhile, less protective effect was observed against erythrocyte damage if fullerenol C<sub>60</sub>(OH)<sub>36</sub> was added after electron irradiation, suggesting the simultaneous production and removal of ROS was critical to inhibiting hemolysis.<sup>11</sup> Nanoparticles can also extend the lifespan of stored blood. Beverly *et al.* found that cerium oxide could protect cells from oxidative stress caused by free radicals generated during storage, reduce cellular damage, biochemical and morphological changes, and slow the decline of ATP. This indicates that nanoparticles can serve as promising drugs for extending the storage time of blood products.<sup>12</sup>

The formation of protein corona on the surface of NPs is another key factor that may reduce their hemolytic activity. Take mesoporous silica nanoparticles (MSNs) as an example. Serum protein adsorption is the first event once NPs enter the bloodstream. According to the adsorption kinetics of the proteins onto MSNs and hemolytic kinetics of erythrocytes induced by MSNs, plasma proteins have a higher affinity and shorter adsorption equilibrium time for MSNs. When MSNs are added into the mixture of proteins and erythrocytes, proteins will be first to be fast adsorbed to the surface of MSNs. After the absorption and formation of protein corona, the hemolysis rate of MSNs is greatly reduced and even no hemolysis occurs.<sup>12</sup> This stable protein corona serves as a very effective protective barrier against the surface charge (positive or negative) of NPs and the

peculiar chemical properties of other surface groups (*e.g.*, silanols, amines, and methylphosphonates), protecting the original microchemical environment of bare nanoparticles and thus reducing hemolysis damage caused by nanoparticles.<sup>13,14</sup>

## 2.2 Influence of nanoparticles on coagulation, thrombosis, and complement activation

In addition to hemolysis, blood compatibility evaluation of NPs also involves the interaction between nanoparticles and other blood visible components such as plasma proteins (fibrinogen, coagulation factor, complement protein), vascular endothelial cells, and platelets,<sup>15</sup> causing a series of biochemical changes such as plasma protein adsorption, coagulation factor activation, platelet activation and adhesion, and then inducing coagulation, thrombosis, and complement activation and other complex blood physiological processes.

The initiation of the coagulation process requires a series of coagulation factors. The mechanism of NPs on coagulation is not completely clear, and the combination of NPs and coagulation factors may affect the steady balance between procoagulation and anticoagulation pathways. Previous studies have fully assessed the effect of NPs on different coagulation pathways by measuring the levels of coagulation factors after NPs treatment. Such NPs as AgNPs and carboxylated polystyrene NPs can inhibit endogenous coagulation factors, while amino-modified polystyrene NPs can activate both endogenous and exogenous coagulation pathways.<sup>16,17</sup> Nanomaterials may adsorb coagulation factors, deprive them of normal biological functions, and then delay clotting time.<sup>18</sup> In addition to coagulation factor assays, activated partial thromboplastin time (APTT), prothrombinogen time (PT) and thrombin time (TT) are also common indicators used to assess the influence of NPs on cascade reaction of endogenous and exogenous coagulation pathways and hemostatic function.<sup>5,19,20</sup> Besides, the structure and conformation of fibrinogen are important for maintaining normal physiological functions during coagulation.<sup>5,20</sup> Currently, nanoparticles have been explored as thrombin cascade activators or anticoagulants,<sup>21,22</sup> such as heparinized mesoporous silica to prolong clotting time,<sup>23</sup> controlled silica-based drug delivery system for “gated” anticoagulation drug release.<sup>24</sup> Other NPs (fullerene, *etc.*) also play an important role in anticoagulation and thrombosis inhibition due to their unique physicochemical properties.<sup>25</sup>

Once nanoparticles enter the bloodstream, the first event is protein adsorption. The type and amount of adsorbed proteins depend on the physicochemical properties of nanoparticles, such as surface charge, chemical groups and scale.<sup>26–28</sup> After protein adsorption, the organism recognizes NPs and activates the immune system to further generate complement cascade activation. Complement activation tests are gaining importance in biosafety evaluation of biomedical materials due to their important role in various biological events such as inflammatory response and coagulation.<sup>27</sup> It has been shown that surface functionalization of NPs can reduce complement activation levels rather than stay clear of the process.<sup>29</sup>



Table 2 Effects of various nanoparticles on oxygen-carrying functions, longevity and membrane oxidative stress of erythrocytes

| Nanoparticles                          | Oxygen-carrying functions                                 |  |                          | longevity related indicators |           |                             |           | Membrane oxidative stress   |           |           |                   |
|--|---|--|--------------------------|------------------------------|-----------|-----------------------------|-----------|-----------------------------|-----------|-----------|-------------------|
|  | Hb  | Oxygen-carrying Band 3                   | PS                       | CD47                         | Caspase-3 | ROS                         | MDA       | SOD/GSH                     | Gpx       | CAT       | Notes             |
| Carbon-based nanoparticles             | Fullerene related NPs <sup>11,25,34,38,39,45</sup>        | Prevent its degradation                  |                          |                              |           |                             |           |                             |           |           | *C <sub>2</sub> N |
|  | Graphene related NPs <sup>4,5,7,8,35,36,44</sup>          |  |                          |                              |           | Increase                    |           |                             |           |           |                   |
|  | Carbon nanotubes <sup>9,10,46</sup>                       |  | Externalization          |                              |           |                             |           |                             |           |           | *AF-SWCNTs        |
| Metal nanoparticles                    | Gold related NPs <sup>29,49,66,80,81</sup>                | Decrease*                                | Induce its aggregation*  | Decrease*                    |           | Increase                    |           |                             |           |           | *PEGylated AuNPs  |
|  | Silver related NPs <sup>29,49,66,80,81</sup>              |  | Externalization          |                              | No effect |                             | Increase  | Increase                    | Increase  | Decrease  | Decrease          |
|  | Titanium dioxide (TiO <sub>2</sub> ) <sup>31,75</sup>     | Specific interactions with Hb skeleton   |                          |                              |           |                             |           |                             |           |           | Increase          |
|  | Fe <sub>3</sub> O <sub>4</sub> magnetic NPs <sup>63</sup> | Interact with Hb                         |                          |                              |           |                             |           |                             |           |           |                   |
| Silica-based nanoparticles             | Silica <sup>12-14,50,78,83-85</sup>                       |  | Externalization          |                              |           | Increase                    |           |                             |           |           | Increase          |
| Instrumentation techniques and methods |   | Surface-enhanced Raman scattering (SERS) | Flow cytometric analysis | Flow cytometry               | Assay kit | Fluorescent probe (DCFH-DA) | Assay kit | Fluorescent probe (DCFH-DA) | Assay kit | Assay kit | Assay kit         |



### 3 NPs interact with erythrocyte membranes

#### 3.1 The way nanoparticles interact with erythrocyte membranes

Finding out about the different ways in which nanoparticles interact with erythrocyte membranes is of great importance for the design of nanoparticle-based drug delivery systems. The relative spatial location of erythrocytes and nanoparticles can be visualized by laser scanning electron microscopy (LSM). Transmission electron microscopy (TEM) mainly focus on the entry information and location information of nanoparticles with erythrocytes. However, due to the fact that different nanoparticles may have similar particle size and electron density, TEM is usually insufficient, and energy filtering transmission electron microscopy (EFTEM) can resolve the issue of chemical compositions of nanoparticles and help study the interaction and structural localization of nanoparticles with erythrocytes in ultrastructural level.<sup>30</sup> Moreover atomic force microscope (AFM),<sup>31</sup> Raman spectroscopy,<sup>32</sup> and confocal fluorescence microscopy are also widely used for such researches. As for the way of molecular dynamics simulation, which shows that electrostatic action, hydrophobic force, Coulomb attraction, and the unique properties of nanoparticles all affect their interaction with the erythrocyte membrane.

Validated by  $^1\text{H}$  pulsed field-gradient NMR technology, the self-diffusion coefficients of the fullerene molecules matched the lateral diffusion coefficients of erythrocyte membrane lipids, suggesting that fullerene derivative molecules can be absorbed by erythrocytes and fixed onto the membrane surface or enter the membrane, with a residence time on erythrocytes of approximately  $440 \pm 70$  ms. Further studies confirmed that

fullerene derivatives can also be taken up by erythrocyte ghost and phosphatidylcholine liposomes.<sup>33</sup> It has also been demonstrated that fullerenes mainly bind to the membrane surface due to the formation of hydrogen bonds, and the removal of fullerenes from the culture medium will cause the dissociation from the cell membrane.<sup>34</sup>

All-atomic molecular dynamics (MD) simulations explored the mechanism by which  $\text{C}_{2}\text{N}$  interacts with erythrocyte membranes and found that the unique electrostatic interaction between  $\text{C}_{2}\text{N}$  with water and membrane produced coulombic resistance (repulsion), which made it difficult for  $\text{C}_{2}\text{N}$  to penetrate the lipid membranes and caused  $\text{C}_{2}\text{N}$  to be adsorbed on the water–membrane interface flatly (Fig. 1b).<sup>7</sup> Meanwhile, Li *et al.* found that  $\text{C}_{2}\text{N}$  had a periodic pore structure and its unique electrostatic potential can adsorb charged amino acids such as lysine and aspartic acid, making itself bind with proteins stably. Such binding was too gentle to destroy the structural integrity of the protein on the erythrocyte membranes.<sup>35</sup> The high biocompatibility of  $\text{C}_{2}\text{N}$  makes it a better drug nanocarrier than other lamellar nanomaterials, such as graphene and molybdenum disulfide. Using *in situ* atomic force microscopy (AFM) imaging, GO was added into the liquid cell of AFM before AFM height images, DMT modulus and adhesion images of lipid bimolecular layers (SBLs) before and after addition were employed for analysis. It was found that GO could peel off single positively charged SBLs and deposit in the hydrophobic region of the lipid bilayer, where free lipid molecules accumulated on the surface of GO to form a lipid–GO–lipid structure. For negatively charged SLBs, GO would deposit only when its concentration was 50 times higher than the original, and neutralizing or reversing the negative charge of SLBs with cations can accelerate the deposition of GO, suggesting that both electrostatic and hydrophobic interactions

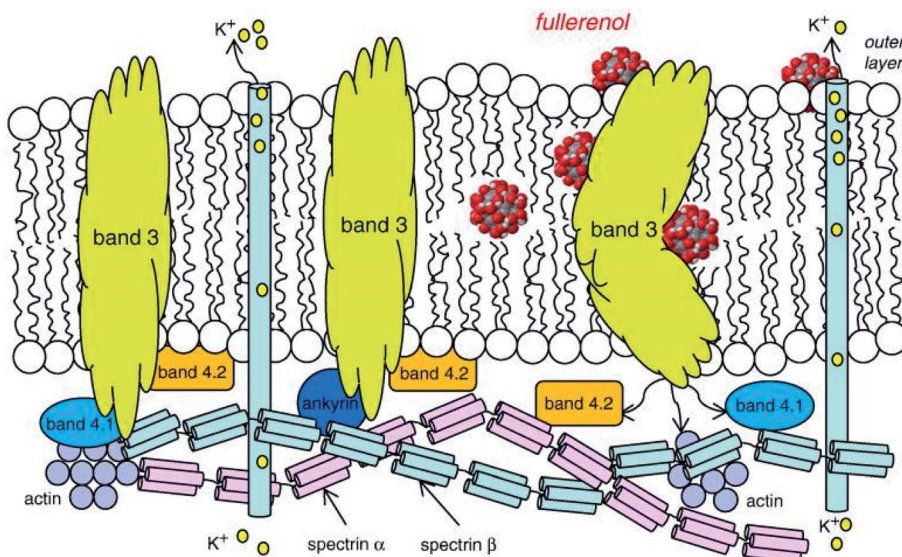


Fig. 2 The interaction of fullerenes and lipid bilayer of erythrocyte membranes. Fullerenes can deposit in the lipid bilayer and bind to band 3 protein to prevent its degradation. And it can also influence the binding sites of other membrane proteins (spectrin, band 4.1, and 4.2 proteins or actin), change the cytoskeleton, and affect erythrocyte morphology. Notes: copyright obtained from ref. 38: (J. Grebowski, A. Krokosz and M. Puchala, *Biochim. Biophys. Acta, Biomembr.*, 2013, **1828**, 2007–2014.). Figure has been reproduced from ref. 38 with permission from the Elsevier, copyright 2021.



play important roles in the way nanoparticles and lipid bilayers interact.<sup>36,37</sup>

### 3.2 Influence of nanoparticles on erythrocyte membrane proteins

Band 3 protein is the dominant protein on the erythrocyte membrane and plays a central role in the formation of the cytoskeleton, and therefore, the conformational changes of band 3 caused by various factors would turn erythrocytes into echinocytes. Polyethylene glycol functionalized gold nanoparticles (PEGylated AuNPs) could induce band 3 accumulation in erythrocytes, which decreased their deformability.<sup>32</sup> Jacek Grebowski *et al.* showed that fullereneol  $C_{60}(OH)_{36}$  could bind to band 3 proteins and prevented proteolytic or ROS-induced band 3 cleavage, affect the binding site of spectrin, band 4.1 and 4.2 proteins or actin, alter the cytoskeleton and affect the morphology of erythrocytes (Fig. 2).<sup>38</sup> They also found that fullereneol  $C_{60}(OH)_{36}$  could interact with functional sites on erythrocyte membranes with available  $-SH$  groups to retain membrane  $-SH$  concentration, increase  $h_w/h_s$  parameters, and

stabilize membrane protein conformation to maintain membrane protein structure and function.<sup>11,39</sup>

Oxidative stress can induce band 3 protein rearrangement on the erythrocyte membrane, and under repeated oxidative perturbations, band 3 clusters progressively grow and shift to an irreversible state.<sup>40</sup> Studies have shown that phagocytic recognition of senescent and oxidatively stressed erythrocytes also appears to be initiated by band 3 clustering, accompanied by bivalent binding of anti-band 3 autoantibodies and oligomerized band 3. At the same time, the production of anti-spectrin autoantibodies also plays an important role in red blood cell clearance.<sup>41,42</sup> However, the biochemistry and mechanisms leading to the formation of band 3 clusters have not been fully determined, but it has been confirmed that the co-interaction of erythrocyte membrane peroxidation and hyperferrous hemoglobin underlies the formation of band 3 clusters.<sup>43</sup> Further studies on the mechanism by which nanoparticle-induced oxidative stress in erythrocytes triggers band 3 accumulation and its effect on erythrocyte longevity remains to be explored.

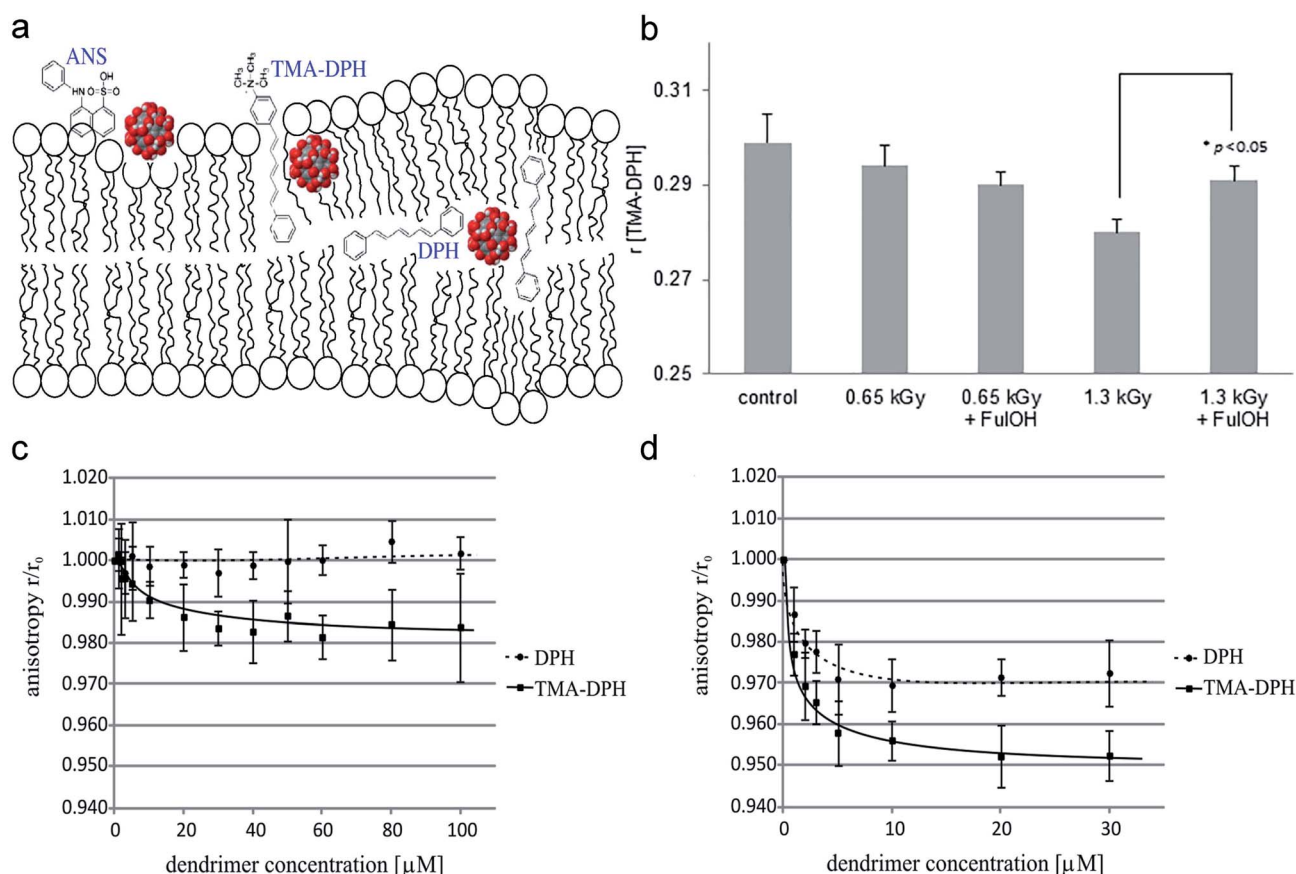


**Fig. 3** (a) The location of ANS, TMA-DPH, DPH in the lipid bilayer. (b) Fullereneol prevented the decrease of the anisotropy coefficient ( $r$ ) for TMA-DPH irradiated with high irradiation doses and then increased the fluidity of erythrocyte membranes. (c and d) Two different dendritic glycopolymers Mal-PEI A (c), Mal-PEI B (d) increased the fluidity of the erythrocyte membrane. Notes: copyright obtained from ref. 11, 34 and 47: (J. Grebowski, P. Kazmierska, G. Litwinienko, A. Lankoff, M. Wolszczak and A. Krokosz, *Biochim. Biophys. Acta, Biomembr.*, 2018, **1860**, 1528–1536. J. Grebowski, A. Krokosz and M. Puchala, *Biochim. Biophys. Acta, Biomembr.*, 2013, **1828**, 241–248. D. Wrobel, A. Janaszewska, D. Appelhans, B. Voit, M. Bryszewska and J. Maly, *Int. J. Pharm.*, 2015, **496**, 475–488.). (a) Has been reproduced from ref. 34 with permission from the Elsevier, copyright 2021. (b) Has been reproduced from ref. 11 with permission from the Elsevier, copyright 2021. (c and d) Has been reproduced from ref. 47 with permission from the Elsevier, copyright 2021.



### 3.3 Influence of nanoparticles on erythrocyte morphology

The interaction of NPs with membrane skeleton proteins can ultimately affect erythrocyte morphology. And such effects also include changes in membrane permeability, integrity, fluidity, and deformability.

The assessment of permeability and integrity of erythrocyte membranes is mainly determined by the amount of potassium in the supernatant, the activity of intracellular enzymes released into the extracellular area (e.g., lactate dehydrogenase), and the hemolysis activity.<sup>11,38,44</sup> Under voltage-clamp conditions, Tatyana *et al.* gave transmembrane currents to double-lipid membranes and added 3  $\mu\text{M}$  fullereneol  $\text{C}_{60}(\text{OH})_{24}$  to both sides of the membrane. They found that fullereneol  $\text{C}_{60}(\text{OH})_{24}$  aggregated in the conductive state and induced ionic permeability of lipid bilayer membranes (BLM) by forming ion pores or transient conductive lipid defects, which is more cations biased. Current trajectories of bilayer lipid membranes incubated with fullereneol show that the current increases with pH and this effect is reversible. Cations such as calcium and magnesium ions can reduce fullereneol  $\text{C}_{60}(\text{OH})_{24}$ -induced potassium ion permeability in the millimolar range.<sup>45</sup> AFSWCNTs can interact directly with the erythrocyte membrane or enter into the cytoplasm, leading to significant membrane damage and phosphatidylserine externalization, which occurs rapidly and is altered in a time- and dose-dependent manner.<sup>46</sup>

The influence of nanoparticles on erythrocyte membranes fluidity was mainly estimated by fluorescence spectroscopy. Different regions of the erythrocyte membrane were labeled with fluorescent probes, such as ANS, DPH, and TMA-DPH, and the anisotropy coefficient ( $r$ ) of each fluorescent probe was calculated to estimate erythrocyte membrane fluidity (Fig. 3a). ANS, DPH, TM-DPH are known to reflect membrane fluidity on the membrane surface, hydrophilic and hydrophobic layers of the lipid bimolecular layer, respectively.<sup>11,34,47</sup> Some researchers used electron spin resonance (ESR) spectroscopy and calculated the ratio of the semi-quantitative parameter low-field peak height to mid-field peak height:  $h_{+1}/h_0$  ratio, to determine the mobility of fatty acid acyl chains in erythrocyte membranes and reflect the mobility of erythrocyte membranes.<sup>39</sup> Grebowski *et al.* incubated fullereneol with erythrocytes at a concentration of 100, 150  $\mu\text{g mL}^{-1}$  for 1 h at 37  $^{\circ}\text{C}$ , and found that anisotropy of ANS, TM-DPH, and DPH was significantly reduced, indicating that the mobility of the erythrocyte membrane in both the inner and outer layers was increased. Fullereneol at high concentrations (150  $\mu\text{g mL}^{-1}$ ) can enter the internal hydrophobic region of the erythrocyte membrane lipid bimolecular layer and then increase the mobility of the inner membrane (Fig. 3a).<sup>34</sup> This result has been also confirmed by the spin-labeling method.<sup>34</sup> However, fullereneol has a protective effect under stress generated by 1.3 kGy high-energy electrons, which may be related to

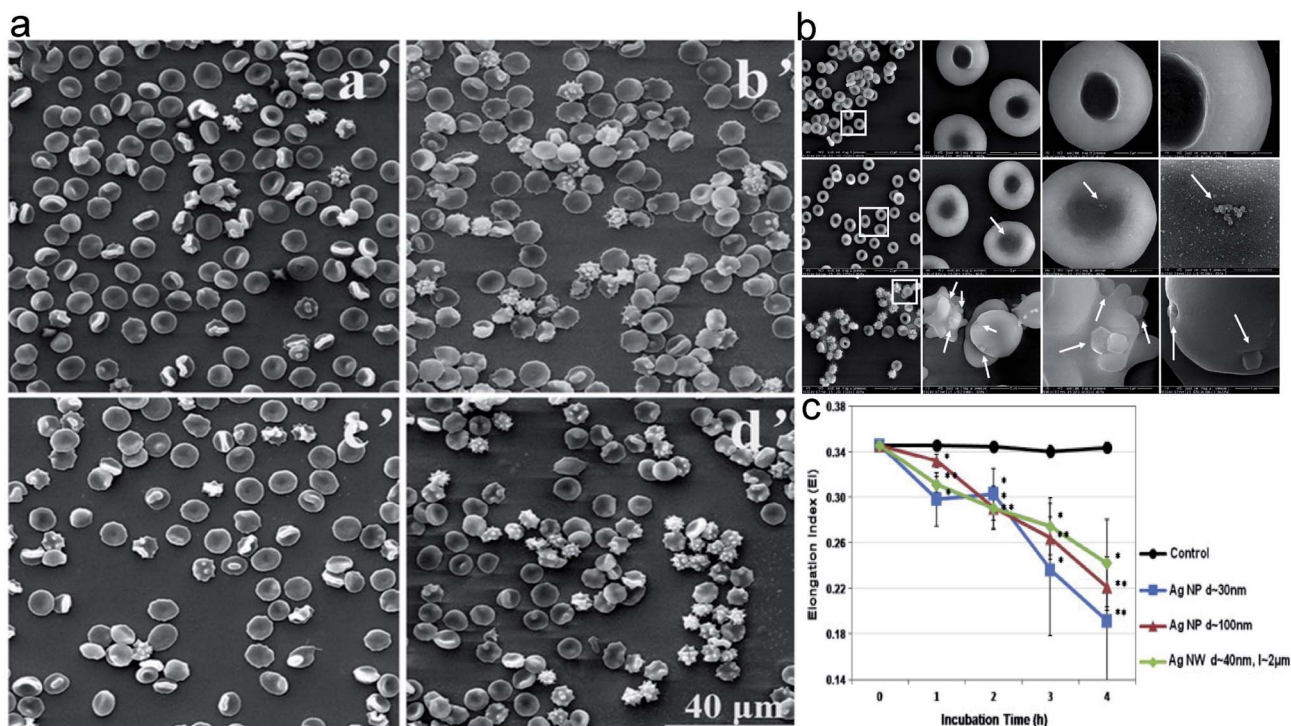


Fig. 4 The morphology of erythrocytes treated with NPs of different size. (a) The SEM images of erythrocytes treated by different-sized PEGylated AuNPs. (a': control; b': 4.5 nm PEGylated AuNPs; c': 13 nm PEGylated AuNPs; d': 30 nm PEGylated AuNPs); (b) The SEM images of erythrocytes treated by different-sized mesoporous silica nanoparticles. (PBS as control (a'), s-MSN (b'), and l-MSN (c')). (c) Elongation index of erythrocytes exposed to silver nanomaterials of different sizes. Notes: copyright obtained from ref. 49, 50 and 51 (Z. He, J. Liu and L. Du, *Nanoscale*, 2014, 6, 9017–9024. Y. Zhao, X. Sun, G. Zhang, B. G. Trewyn, I. I. Slowing and V. S.-Y. Lin, *ACS Nano*, 2011, 5, 1366–1375. M. J. Kim and S. Shin, *Food Chem. Toxicol.*, 2014, 67, 80–86.). (a) Has been reproduced from the ref. 49 with permission from The Royal Society Chemistry, copyright 2021. (b) Has been reproduced from the ref. 50 with permission from American Chemical Society, copyright 2021. (c) Has been reproduced from the ref. 51 with permission from the Elsevier, copyright 2021.



the scavenging of reactive oxygen and the altered interaction of fullerene with damaged membrane structures (Fig. 3b).<sup>11</sup> Wrobel *et al.* found that dendritic glycopolymer dendrimer also reduces the *R*-values of DPH and TM-DPH, causing lipid recombination on erythrocyte membranes to increase membrane mobility (Fig. 3c and d).<sup>47</sup>

Erythrocyte deformation is one of the important factors that affects the apparent viscosity of blood and the effective perfusion of microcirculation *in vivo*. It is also an important determinant of erythrocyte lifespan, constituting the fundamental feature of its biological function. The erythrocyte membrane skeleton blocks the transformation of normal biconcave disc-like erythrocytes into spiny erythrocytes by fixing transmembrane proteins,<sup>48</sup> so NPs that interact with erythrocyte membrane skeleton proteins can also affect erythrocytes and convert them into echinocytosis.<sup>35,49</sup> Previous studies have shown that the ability of NPs to regulate erythrocyte deformation is usually associated with the way in which NPs interact with the erythrocyte membrane.<sup>44</sup> According to the study by He *et al.*, the deformability of erythrocytes decreased after interacting with PEGylated AuNPs, and the scanning electron microscopy (SEM) images showed that large-sized PEGylated AuNPs were attached to the erythrocytes membrane, causing strong local membrane deformation and inducing the transformation into echinocytic shape. Thus, they speculated that the reduced deformation capacity of erythrocytes membrane might be due to the fact that PEGylated AuNPs were attached to the erythrocyte surface and limited the elasticity of the cell membrane (Fig. 4a).<sup>49</sup> Zhao *et al.* reported that erythrocytes exposed to silica nanoparticles significantly reduced deformation capacity. Large MSNs (L-MSNs, *c.a.* 600 nm) were more likely to be absorbed onto the erythrocyte, causing a strong local deformation of the cell membrane to package these nanoparticles (Fig. 4b). After enveloping L-MSNs, the cell membrane underwent echinocerebral-like changes, resulting in a decrease of the ratio of surface area to volume (*S/V*) of erythrocytes. It is well known that the *S/V* ratio is a determinant of erythrocyte deformation capacity, and the cell deformation capacity will be significantly reduced if the *S/V* ratio is slightly reduced. They found that this might be due to the higher binding energy ( $E_i$ ) that resulted from the larger external area of L-MSNs, which overcame the free energy required to bend to the membrane and adapt to the surface of the MSNs, pulling the cell membrane towards the surface of the nanoparticles.<sup>50</sup> Unlike MSNs, Ag-NPs had a particle size that exerted an opposite effect on erythrocyte deformation capacity. Namely, smaller Ag-NPs with the size of *c.a.* 30 nm have a greater effect on erythrocyte deformation capacity than larger ones (*c.a.* 100 nm) (Fig. 4c).<sup>51</sup> Metal nanoparticles containing cations induce structural changes in the lipid bimolecular layer of the erythrocyte membrane, leading to an increase in the microviscosity of the cell membrane and the rupture of swollen erythrocytes.<sup>52</sup> Disorders of erythrocyte membrane integrity may further exacerbate oxidative stress, which is closely associated with many diseases, such as cardiovascular diseases, ischemic diseases, and diabetes.

## 4 Nanoparticles affect erythrocyte longevity and function

### 4.1 Erythrocyte longevity

Erythrocytes have a lifespan of approximately 100–120 days after being released from bone marrow. Nearing the end of their life cycle or being damaged by some factors, erythrocytes will express some unique signals that activate macrophages to induce phagocytosis. According to current views on erythrocyte–macrophage interactions, the phagocytosis of erythrocytes depends on the net positive and negative signals it sends to macrophages. The mechanisms by which macrophage clears senescent or damaged erythrocytes include the following: band 3-mediated erythrocyte clearance, phosphatidylserine (PS)-mediated erythrocyte clearance, and CD47-mediated erythrocyte clearance (Fig. 5).<sup>53,54</sup> The regulatory effects of autoantibodies and subsequent complement binding may provide positive signals for the activation of macrophages.<sup>55,56</sup> For example, anti-band 3 autoantibodies produced by aging or oxidative stress can bind to band 3 on the erythrocyte membrane and promote macrophage phagocytosis through the Fc receptor of macrophages.<sup>42</sup> By contrast, membrane components such as CD47 and salivary acid emit negative signals that inhibit macrophages from phagocytic responses.<sup>55,57,58</sup> Thus, the shortened erythrocyte lifespan may be due to an enhanced positive signal, a weakened negative signal, or a simultaneous change in both signals.

According to previous studies, little is known about the mechanism by which NPs induced erythrocyte death. It is speculated that suppression of CD47 molecule on the erythrocyte membrane, exposure to phosphatidylserine, increased intracellular calcium concentration, and activating calpain are probably the ways that NPs reduces erythrocyte longevity.<sup>49,59</sup> CD47 is known as integrin associated protein belonging to the immunoglobulin superfamily, it is also a ligand for signal-regulated protein  $\alpha$  (SIRP $\alpha$ ) and CD47 and SIRP $\alpha$  together constitute the CD47-SIRP $\alpha$  signaling system. The interaction between CD47 molecules and SIRP $\alpha$  receptors on macrophages prevents the phagocytosis of erythrocytes by macrophages. Thus, either a reduction or defect in CD47 may increase erythrocytes clearance, determining erythrocyte longevity.<sup>57,60,61</sup> One study found that co-incubation with PEGylated AuNPs and erythrocyte resulted in decreased CD47 expression on erythrocyte membranes and the effect was more pronounced in the case of greater particle size, suggesting that PEGylated AuNPs may affect erythrocyte survival *in vivo* by affecting CD47 expression.<sup>50</sup> The CD47 molecule is also regulated by the shape and rigidity of erythrocytes and in turn regulates the phagocytosis behavior,<sup>62</sup> so the changes in erythrocyte morphology induced in each case may affect erythrocyte longevity. Phosphatidylserine plays a key role in cell cycle signaling and is closely related to apoptosis. When exposed to Fe<sub>3</sub>O<sub>4</sub> magnetic nanoparticles (Fe<sub>3</sub>O<sub>4</sub>-MNP) *in vitro*, phosphatidylserine on the erythrocyte is transferred outside the cell membrane, recognized by specific phagocytic receptors before macrophage phagocytosis and degradation occurs. Phosphatidylserine



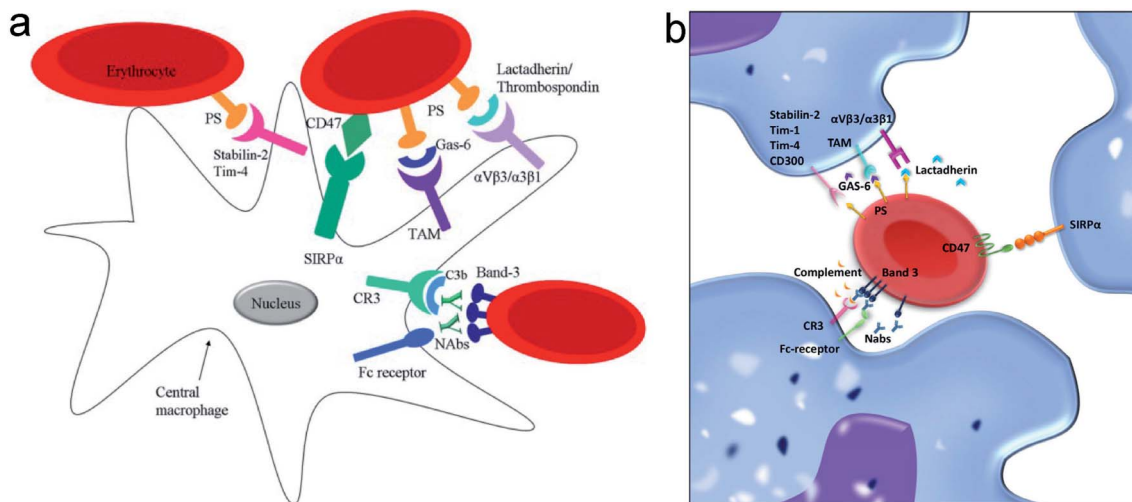


Fig. 5 (a and b) The positive and negative signals involved in the interaction between macrophages and red blood cell (RBC) regulating clearance. Notes: copyright obtained from ref. 53 and 54 (D. Z. de Back, E. B. Kostova, M. van Kraaij, T. K. van den Berg and R. van Bruggen, *Front. Physiol.*, DOI: 10.3389/fphys.2014.00009. T. R. L. Klei, S. M. Meinderts, T. K. van den Berg and R. van Bruggen, *Front. Immunol.*, DOI: 10.3389/fimmu.2017.00073.). (a) Has been reproduced from the journal, *Front. Physiol.*, with open access. (b) Has been reproduced from the journal, *Front. Immunol.*, with open access.

externalization is determined to be more sensitive than classical hemolysis tests in evaluation of hemocompatibility, suggesting that exogenous phosphatidylserine can be a predictive factor.<sup>63</sup> Polyvinylpyrrolidone and citrate-coated AgNPs (PVP-AgNPs and CT-AgNPs) resulted in significant and dose-dependent increases in intracellular  $\text{Ca}^{2+}$  and Annexin V concentrations, and increased intracellular calcium further activated calpains, which played a role in erythrocyte apoptosis. Although the presence of caspases in erythrocytes has been well established, their role in erythrocyte apoptosis has not been clearly defined.<sup>59</sup> Berg *et al.* argued that although mature erythrocytes contain a considerable amount of caspase-3 and -8, various pro-apoptotic stimuli fail to activate them in intact erythrocytes, while incubation of cytosolic extracts of RBCs with exogenous caspases leads to functionally active of caspase-3 and -8 *in vitro*. This may be due to the fact that erythrocytes lack other essential components of mitochondrial apoptotic cascade such as caspase-9, Apaf-1, and cytochrome c.<sup>64</sup>

$\text{Ag}^+$  at low concentrations could induce erythrocyte death *in vitro*. Sopjani *et al.* found that like apoptosis in nucleated cells, erythrocyte death was characterized by cell shrinkage and cell membrane scrambling by phosphatidylserine exposure. However, the mechanism of  $\text{Ag}^+$  induced erythrocyte death cannot be explained by the increase in intracellular calcium ion concentration and ceramide it may be triggered by ATP depletion, depletion of cellular NO concentration, and activation of protein kinase C.<sup>65</sup>

#### 4.2 Oxygen-carrying and oxygen-releasing functions of erythrocytes

The primary function of erythrocytes is to transport oxygen and carbon dioxide. Hemoglobin (Hb) is an important component of erythrocytes, and in the reduced state, Hb binds oxygen to form oxygenated hemoglobin, which transports oxygen to various tissues and organs to provide energy for the maintenance of normal life activities. Changes in the composition,

amino acid residues, spatial structure of Hb can affect its function. Many factors affect oxygen transport, including pH, temperature, 2,3-diphosphoglycerate.

The dissociation capacity of oxygen transported to the target organ by erythrocytes can be reflected by the oxygen dissociation curve. PEGylated AuNPs can reduce the content of  $\text{P}_{50}$  in erythrocytes, increase the content of methemoglobin, reduce the oxygen-binding capacity of erythrocytes, and thus affect the oxygen-carrying function of erythrocytes.<sup>49</sup> Spectroscopic techniques are usually used to study the interaction between NPs and Hb.<sup>66–68</sup> According to resonance light scattering spectroscopy, polymerization occurred between silver nanoparticles (nanoAg) and Hb, and circular dichroism (CD) spectroscopy showed that polymerization triggered the loss of Hb  $\alpha$ -helix content, suggesting that at the molecular level, AgNP was more toxic to Hb secondary structures and might lead to a severe loss of biological activity.<sup>69</sup> Furthermore, AgNP induced a dynamic conversion from  $\alpha$ -helix to  $\beta$ -sheet, resulting in structural deformation of Hb. Due to the electrostatic interaction between positively charged Hb and negatively charged Ag NP, Hb protein corona would be formed on the surface of Ag NP, and the secondary structural changes from  $\alpha$ -helix to  $\beta$ -fold depended on the time taken by corona formation (Fig. 6).<sup>68</sup> Surface-enhanced Raman (SERS) is used as a local probe for the NP environment, and it can provide insights at the molecular level into the processes associated with nanoparticle-induced structural changes in the lipid bimolecular layer, Hb conformation changes, *etc.* Since proteins interact with different nanoparticles which have different materials, surface ligands, and size, SERS spectra information is strongly dependent on the type of nanoparticles.<sup>66,67</sup>

#### 4.3 Antioxidant function of erythrocytes

Reactive oxygen species (ROS) consists of superoxide radicals ( $\cdot\text{O}_2^-$ ), hydrogen peroxide ( $\text{H}_2\text{O}_2$ ), hydroxyl radicals ( $\cdot\text{OH}$ ), *etc.*



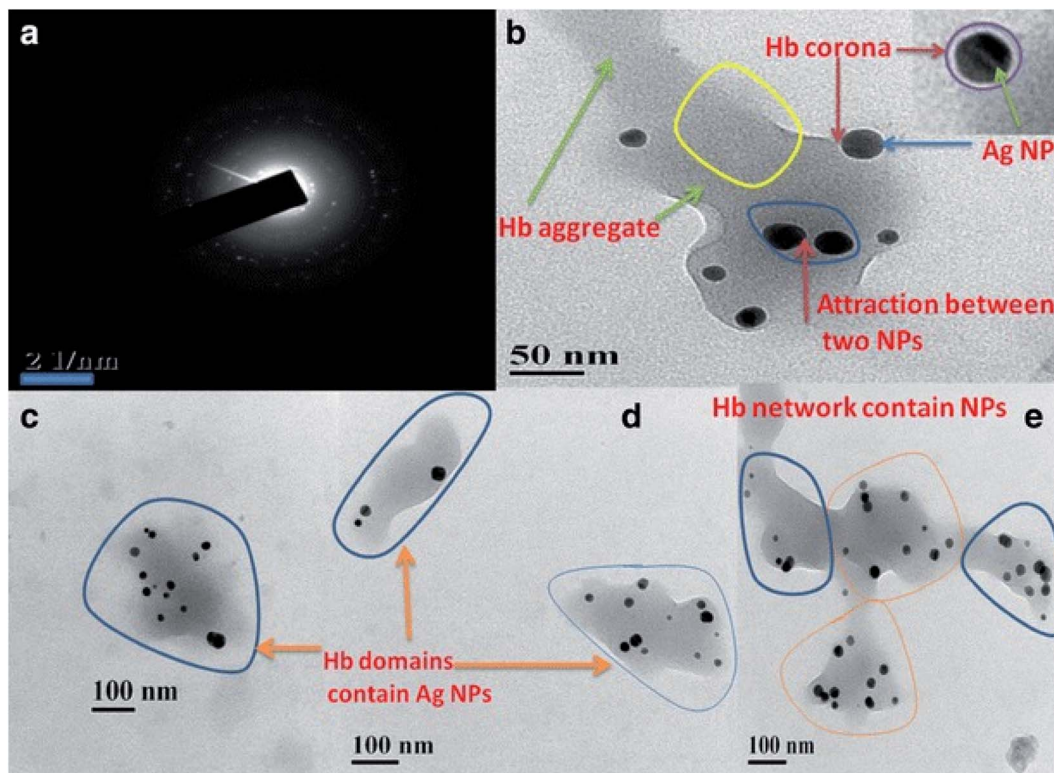


**Fig. 6** (a) SAED pattern of Hb–Ag corona. (b) TEM showed aggregation of Hb after coat over the Ag NP with an even, thin Hb corona. (c and d) Three different Hb domains contain AgNPs. (e) Different domains of Hb containing AgNPs (dark spots) and AgNPs aggregates are connecting each other to form Hb network. Notes: copyright obtained from ref. 68: (A. K. Bhunia, T. Kamilya and S. Saha, *Nano Convergence*, 2017, 4, 28.). Figure has been reproduced from the journal, *Nano Convergence*, with open access.

Mitochondria are the main organelles that produce ROS. As ROS can be decomposed and transformed into harmless molecules by intracellular enzymes such as SOD and CAT, erythrocytes are vulnerable to foreign toxicants because of their inability to synthesize these enzymes. Oxidative damage to erythrocytes mainly manifests itself in increased protein fragmentation, increased protein carbonylation and (non-)enzymatic glycosylation, membrane lipid peroxidation, and band 3 cluster accumulation.<sup>70,71</sup> These changes further cause changes and rupture to the shape of erythrocytes.

The antioxidant defense of erythrocytes involves several erythrocyte-associated biomolecules, including superoxide dismutase (SOD), catalase (CAT), glutathione peroxidase (GPX), glutathione (GSH), and malondialdehyde (MDA).<sup>72–74</sup> It was shown that AgNPs affect both the erythrocyte enzymatic (SOD/CAT/GPX) and non-enzymatic antioxidant systems (GSH/MDA), reducing the antioxidant function of erythrocytes. Further mechanism exploration indicated that direct intermolecular interaction is one of the important catalysts to the changes in antioxidant enzyme activity after exposure to NPs at the cellular level. According to spectroscopic analysis, the mechanism of interaction and conformational changes at the molecular level after direct exposure of enzyme protein to AgNPs are also important factors influencing its activity.<sup>67</sup> Lipid peroxidation products exert deleterious effects on cell membranes and the main product, MDA, has been widely used

as a marker of lipid peroxidation and oxidative stress.<sup>49,74,75</sup> Due to the overproduction of ROS, erythrocytes exposed to PEGylated AuNPs had elevated MDA levels and in turn the oxidative stress occurred on the cells.<sup>43</sup> Li and Sahoo *et al.* demonstrated the dose-dependent effect of the severity of lipid peroxidation of cell membrane with nanoparticles,<sup>74,75</sup> which may further disrupt their fluidity, permeability, deformability, and shorten the lifespan of erythrocytes.

#### 4.4 Hemorheology

Minor alterations in blood rheological features can lead to circulatory diseases of the microvascular system, and rheology can indirectly reflect erythrocyte function by detecting several parameters that reflect changes in erythrocyte membrane morphology and structure.<sup>48,50,51</sup> With the development of this technology, the rheological properties of blood components such as erythrocyte membrane skeletal proteins and membrane phospholipids on erythrocyte rheology can be studied at the molecular level in recent years. However, these changes in blood rheological properties are rarely used in nanotoxicological assessment.

The detection of hematological rheology indicators such as erythrocyte deformation index, rigidity index, and aggregation index can help us gain keen insights into the interactions between nanoparticles and erythrocytes to evaluate the severity of nanoparticle cytotoxicity.<sup>76–78</sup> Ran *et al.* found that Fe<sub>3</sub>O<sub>4</sub>-



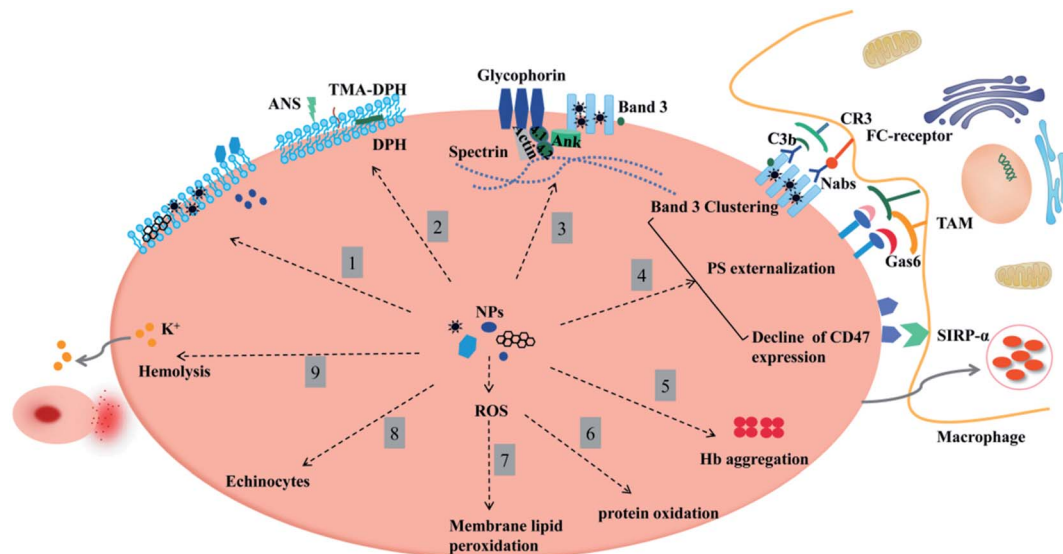


**Fig. 7** An overview of nanomaterials affecting the morphology, structure, and function of erythrocytes. Clockwise: (1) interaction of nanoparticles with the erythrocyte membrane in three ways: nanoparticles are attached flatly to the surface, inserted or deposited into the lipid bilayer, cross the cell membrane and enter the cell. (2) Nanoparticles affect the mobility of erythrocytes. (3) Nanoparticles target membrane structural proteins, causing band 3 protein cluster and cleavage and affecting the binding site of spectrin, band 4.1, and 4.2 proteins or actin. Band 3 (AE1) also indirectly affects Hb-oxygen affinity by regulating ionic homeostasis. (4) Nanoparticle-erythrocyte interaction promotes membrane accumulation of band 3 clusters, PS exposure in the outer leaflet, and the decline of CD47 expression, which are positive signals that macrophage phagocytosis is stimulated. (5) Nanoparticle-erythrocyte interaction promotes Hb aggregation and the formation of corona (loss of Hb  $\alpha$ -helix content or a dynamic shift from  $\alpha$ -helix to  $\beta$ -fold). (6 and 7) Nanoparticle-erythrocyte interaction affects protein and membrane lipid peroxidation. (8 and 9) All of these alterations will affect membrane deformability, increase the osmotic fragility of erythrocytes, promote the formation of vesiculations and echinocytes, and finally, leave red blood cells ruptured and hemolyzed.

MNPs significantly affected indicators of mechanical properties of erythrocytes, such as erythrocyte deformation index, rigidity index, aggregation index, and erythrocyte electrophoresis time, but little is known about the mechanism.<sup>63</sup> The shape, size, concentration, surface modification, and incubation time of the nanoparticles significantly affected the deformation index and aggregation index of erythrocytes under the same shear stress conditions.<sup>51,77,78</sup> These indicators are closely related to the structure and morphology of erythrocyte membranes, function and longevity of erythrocytes, and can induce eryptosis and changes in blood flow characteristics. At the same time, the assessment of blood viscosity can also facilitate the early diagnosis of diseases that may be caused by nanoparticle cytotoxicity.

Hemorheology can also be used to evaluate the effects of nanoparticles on blood clotting and thrombosis and help to explore their mechanisms. Steuer and colleagues employed oscillation shear rheometry to study the effects of zinc oxide and silica nanoparticles on the formation of whole blood thrombosis. They found that nanoparticles with negatively charged surfaces (e.g., silica) and isoelectric points below plasma pH induced blood clotting at high concentrations, and in contrast, positively charged zinc oxide had anticoagulant effects. However, at low concentrations, both types of particles induced strong coagulation, and it is clear that this biological effect is not simply due to the surface charge. The possible reason is that after nanoparticles' entry into the blood, the package by plasma protein brings a similar face to nanoparticles, which in turn triggers the procoagulant effect.<sup>79</sup>

## 5 Summary and outlook

Blood is regarded as a flowing connective tissue that delivers chemicals for diagnostic or therapeutic purposes to target organs. In general, we should minimize the harmful effects of chemical drugs on blood cells. It is recommended that nanoparticles, which are widely used in the field of biomedicine, be evaluated for the safety of cells, especially red blood cells when they enter the body. Current studies on interactions between nanoparticles and erythrocytes are primarily dependent on hemolytic evaluation, with few studies taking account of structure and function changes of erythrocytes themselves, as hemolysis does not fully reflect the damages to erythrocytes. Therefore, this paper focuses on the effects of nanoparticles on the structure and function of erythrocyte membranes and the underlying mechanisms. This study is expected to find some regularities based on experiments in order to help improve the NPs safety *in vivo* and contribute to the development of new nanodrugs or nanocarriers. One final point to be mentioned is the purity of nanomaterials that should be paid more attention to, for the impurities involved during the synthesis would impart some drastic effects on erythrocytes (Fig. 7).

Altogether, there are three ways in which NPs act on erythrocyte membranes, namely, attachment to the membrane surface, insertion into the membrane or entrance into the cell according to the different chemical properties. NPs interact with skeletal proteins on the erythrocyte membrane (such as band 3, spectrin, etc.), affect the protein content and conformation, further change the integrity, permeability, mobility,



and deformability of the erythrocyte membrane, cause erythrocyte rupture and hemolysis, increase erythrocyte aggregation or reduce deformation ability. At the same time, the interactions between nanoparticles and erythrocytes will produce ROS and induce oxidative stress, leading to some biological changes such as oxidation of membrane proteins and lipid peroxidation, affecting the homeostasis of erythrocyte membranes and causing hemolysis and other adverse reactions that prevent erythrocytes from performing their normal biological functions. Membrane disorders of any cause may probably shorten erythrocyte lifespan through membrane surface molecules (CD47, band 3, phosphatidylserine, etc.).

In summary, a more in-depth investigation of the effect of nanoparticles on red blood cells is critical to studies on the hemocompatibility of nanomaterials and nano-toxicology. As the process of applying nanotechnology-based achievements to industrialized and commercial production was noticeably accelerated, it is necessary to develop more advanced and accurate evaluations of hemocompatibility, which might be of great importance to induce the complications involved in hematology and improve the biosafety of nanomaterials. This paper is expected to provide guidance for the development of new nanodrugs and nanocarriers for disease treatment in the future.

## Conflicts of interest

There are no conflicts to declare.

## Acknowledgements

Project was supported by the Foundation of 20-163-15-ZD-006-002-04.

## References

- I. Khan, K. Saeed and I. Khan, *Arabian J. Chem.*, 2019, **12**, 908–931.
- H. Su, Y. Wang, Y. Gu, L. Bowman, J. Zhao and M. Ding, *J. Appl. Toxicol.*, 2018, **38**, 3–24.
- K. de la Harpe, P. Kondiah, Y. Choonara, T. Marimuthu, L. du Toit and V. Pillay, *Cells*, 2019, **8**, 1209.
- K.-H. Liao, Y.-S. Lin, C. W. Macosko and C. L. Haynes, *ACS Appl. Mater. Interfaces*, 2011, **3**, 2607–2615.
- R. Feng, Y. Yu, C. Shen, Y. Jiao and C. Zhou, *J. Biomed. Mater. Res.*, 2015, **103**, 2006–2014.
- X. Zhang, J. Yin, C. Peng, W. Hu, Z. Zhu, W. Li, C. Fan and Q. Huang, *Carbon*, 2011, **49**, 986–995.
- L. Liu, S. Zhang, L. Zhao, Z. Gu, G. Duan, B. Zhou, Z. Yang and R. Zhou, *Small*, 2018, **14**, 1803509.
- Y. Wang, B. Zhang and G. Zhai, *RSC Adv.*, 2016, **6**, 68322–68334.
- S. V. Prylutska, I. I. Grynuk, O. P. Matyshevska, V. M. Yashchuk, Yu. I. Prylutsky, U. Ritter and P. Scharff, *Phys. E*, 2008, **40**, 2565–2569.
- Y. Heo, C.-A. Li, D. Kim and S. Shin, *Clin. Hemorheol. Microcirc.*, 2017, **65**, 49–56.
- J. Grebowski, P. Kazmierska, G. Litwinienko, A. Lankoff, M. Wolszczak and A. Krokosz, *Biochim. Biophys. Acta, Biomembr.*, 2018, **1860**, 1528–1536.
- Z. Ma, J. Bai, Y. Wang and X. Jiang, *ACS Appl. Mater. Interfaces*, 2014, **6**, 2431–2438.
- J. Shi, Y. Hedberg, M. Lundin, I. Odnevall Wallinder, H. L. Karlsson and L. Möller, *Acta Biomater.*, 2012, **8**, 3478–3490.
- A. J. Paula, D. S. T. Martinez, R. T. Araujo Júnior, A. G. Souza Filho and O. L. Alves, *J. Braz. Chem. Soc.*, 2012, **23**, 1807–1814.
- T. M. Potter, J. C. Rodriguez, B. W. Neun, A. N. Ilinskaya, E. Cedrone and M. A. Dobrovolskaia, in *Characterization of Nanoparticles Intended for Drug Delivery*, ed S. E. McNeil, Springer New York, New York, NY, 2018, vol. 1682, pp. 103–124.
- F. Martínez-Gutierrez, E. P. Thi, J. M. Silverman, C. C. de Oliveira, S. L. Svensson, A. V. Hoek, E. M. Sánchez, N. E. Reiner, E. C. Gaynor, E. L. G. Pryzdial, E. M. Conway, E. Orrantia, F. Ruiz, Y. Av-Gay and H. Bach, *Nanomedicine*, 2012, **8**, 328–336.
- C. Oslakovic, T. Cedervall, S. Linse and B. Dahlbäck, *Nanomedicine*, 2012, **8**, 981–986.
- J.-Y. Yang, J. Bae, A. Jung, S. Park, S. Chung, J. Seok, H. Roh, Y. Han, J.-M. Oh, S. Sohn, J. Jeong and W.-S. Cho, *PLoS One*, 2017, **12**, e0181634.
- H. Huang, W. Lai, M. Cui, L. Liang, Y. Lin, Q. Fang, Y. Liu and L. Xie, *Sci. Rep.*, 2016, **6**, 25518.
- X. Liu and J. Sun, *J. Nanosci. Nanotechnol.*, 2013, **13**, 222–228.
- C. F. Greineder, M. D. Howard, R. Carnemolla, D. B. Cines and V. R. Muzzykantor, *Blood*, 2013, **122**, 1565–1575.
- C. L. Modery-Pawłowski, H.-H. Kuo, W. M. Baldwin and A. S. Gupta, *Nanomedicine*, 2013, **8**, 1709–1727.
- C. Argyo, V. Cauda, H. Engelke, J. Rädler, G. Bein and T. Bein, *Chem. - Eur. J.*, 2012, **18**, 428–432.
- R. Bhat, À. Ribes, N. Mas, E. Aznar, F. Sancenón, M. D. Marcos, J. R. Murguía, A. Venkataraman and R. Martínez-Mañez, *Langmuir*, 2016, **32**, 1195–1200.
- S. Xia, J. Li, M. Zu, J. Li, J. Liu, X. Bai, Y. Chang, K. Chen, W. Gu, L. Zeng, L. Zhao, G. Xing and G. Xing, *Nanomedicine*, 2018, **14**, 929–939.
- C. Fornaguera, G. Calderó, M. Mitjans, M. P. Vinardell, C. Solans and C. Vauthier, *Nanoscale*, 2015, **7**, 6045–6058.
- S. Li, Z. Guo, Y. Zhang, W. Xue and Z. Liu, *ACS Appl. Mater. Interfaces*, 2015, **7**, 19153–19162.
- C. Vauthier, B. Persson, P. Lindner and B. Cabane, *Biomaterials*, 2011, **32**, 1646–1656.
- Q. H. Quach, R. L. X. Kong and J. C. Y. Kah, *Bioconjugate Chem.*, 2018, **29**, 976–981.
- B. M. Rothen-Rutishauser, S. Schürch, B. Haenni, N. Kapp and P. Gehr, *Environ. Sci. Technol.*, 2006, **40**, 4353–4359.
- M. Ghosh, A. Chakraborty and A. Mukherjee, *J. Appl. Toxicol.*, 2013, **33**, 1097–1110.
- M. A. G. Soler, S. N. Bão, G. B. Alcântara, V. H. S. Tibúrcio, G. R. Paludo, J. F. B. Santana, M. H. Guedes, E. C. D. Lima, Z. G. M. Lacava and P. C. Morais, *J. Nanosci. Nanotechnol.*, 2007, **7**, 1069–1071.



- 33 I. Avilova, E. Khakina, O. Kraevaya, A. Kotelnikov, R. Kotelnikova, P. Troshin and V. Volkov, *Biochim. Biophys. Acta, Biomembr.*, 2018, **1860**, 1537–1543.
- 34 J. Grebowski, A. Krokosz and M. Puchala, *Biochim. Biophys. Acta, Biomembr.*, 2013, **1828**, 241–248.
- 35 B. Li, W. Li, J. M. Perez-Aguilar and R. Zhou, *Small*, 2017, **13**, 1603685.
- 36 X. Liu and K. L. Chen, *Langmuir*, 2015, **31**, 12076–12086.
- 37 X. Hu, H. Lei, X. Zhang and Y. Zhang, *Microsc. Res. Tech.*, 2016, **79**, 721–726.
- 38 J. Grebowski, A. Krokosz and M. Puchala, *Biochim. Biophys. Acta, Biomembr.*, 2013, **1828**, 2007–2014.
- 39 J. Grebowski and A. Krokosz, *J. Spectrosc.*, 2015, **2015**, 1–6.
- 40 H. Shimo, S. N. V. Arjunan, H. Machiyama, T. Nishino, M. Suematsu, H. Fujita, M. Tomita and K. Takahashi, *PLoS Comput. Biol.*, 2015, **11**, e1004210.
- 41 R. Hornig and H. U. Lutz, *Exp. Gerontol.*, 2000, **35**, 1025–1044.
- 42 H. U. Lutz, *Transfus. Med. Hemotherapy*, 2012, **39**, 321–327.
- 43 N. Arashiki, N. Kimata, S. Manno, N. Mohandas and Y. Takakuwa, *Biochemistry*, 2013, **52**, 5760–5769.
- 44 A. Sasidharan, L. S. Panchakarla, A. R. Sadanandan, A. Ashokan, P. Chandran, C. M. Girish, D. Menon, S. V. Nair, C. N. R. Rao and M. Koyakutty, *Small*, 2012, **8**, 1251–1263.
- 45 T. I. Rokitskaya and Y. N. Antonenko, *Biochim. Biophys. Acta, Biomembr.*, 2016, **1858**, 1165–1174.
- 46 S. Sachar and R. K. Saxena, *PLoS One*, 2011, **6**, e22032.
- 47 D. Wrobel, A. Janaszewska, D. Appelhans, B. Voit, M. Bryszewska and J. Maly, *Int. J. Pharm.*, 2015, **496**, 475–488.
- 48 S. Svetina, *Cell. Mol. Biol. Lett.*, 2012, **17**, 171–181.
- 49 Z. He, J. Liu and L. Du, *Nanoscale*, 2014, **6**, 9017–9024.
- 50 Y. Zhao, X. Sun, G. Zhang, B. G. Trewyn, I. I. Slowing and V. S.-Y. Lin, *ACS Nano*, 2011, **5**, 1366–1375.
- 51 M. J. Kim and S. Shin, *Food Chem. Toxicol.*, 2014, **67**, 80–86.
- 52 A. I. Kozelskaya, A. V. Panin, I. A. Khlusov, P. V. Mokrushnikov, B. N. Zaitsev, D. I. Kuzmenko and G. Y. Vasyukov, *Toxicol. in Vitro*, 2016, **37**, 34–40.
- 53 D. Z. de Back, E. B. Kostova, M. van Kraaij, T. K. van den Berg and R. van Bruggen, *Front. Physiol.*, 2014, **5**, 9.
- 54 T. R. L. Klei, S. M. Meinderts, T. K. van den Berg and R. van Bruggen, *Front. Immunol.*, 2017, **8**, 73.
- 55 H. U. Lutz, *Cell. Mol. Biol.*, 2004, **50**(2), 107–116.
- 56 H. U. Lutz, *Naturally Occurring Antibodies (NABs)*, 2012, **750**, 76–90.
- 57 Y. Murata, T. Kotani, H. Ohnishi and T. Matozaki, *J. Biochem.*, 2014, **155**, 335–344.
- 58 S. Khandelwal, N. van Rooijen and R. K. Saxena, *Transfusion*, 2007, **47**, 1725–1732.
- 59 Z. Ferdous, S. Beegam, S. Tariq, B. H. Ali and A. Nemmar, *Cell. Physiol. Biochem.*, 2018, **49**, 1577–1588.
- 60 M. Olsson and P.-A. Oldenburg, *Blood*, 2008, **112**, 4259–4267.
- 61 T. Ishikawa-Sekigami, Y. Kaneko, Y. Saito, Y. Murata, H. Okazawa, H. Ohnishi, P.-A. Oldenburg, Y. Nojima and T. Matozaki, *Biochem. Biophys. Res. Commun.*, 2006, **343**, 1197–1200.
- 62 N. G. Sosale, T. Rouhiparkouhi, A. M. Bradshaw, R. Dimova, R. Lipowsky and D. E. Discher, *Blood*, 2015, **125**, 542–552.
- 63 Q. Ran, Y. Xiang, Y. Liu, L. Xiang, F. Li, X. Deng, Y. Xiao, L. Chen, L. Chen and Z. Li, *Sci. Rep.*, 2015, **5**, 16209.
- 64 C. P. Berg, I. H. Engels, A. Rothbart, K. Lauber, A. Renz, S. F. Schlosser, K. Schulze-Osthoff and S. Wesselborg, *Cell Death Differ.*, 2001, **8**, 1197–1206.
- 65 M. Sopjani, M. Föller, J. Haendeler, F. Götz and F. Lang, *J. Appl. Toxicol.*, 2009, **29**, 531–536.
- 66 D. Drescher, T. Büchner, D. McNaughton and J. Kneipp, *Phys. Chem. Chem. Phys.*, 2013, **15**, 5364.
- 67 Y. Kang, M. Si, Y. Zhu, L. Miao and G. Xu, *Spectrochim. Acta, Part A*, 2013, **108**, 177–180.
- 68 A. K. Bhunia, T. Kamilya and S. Saha, *Nano Convergence*, 2017, **4**, 28.
- 69 Z. Chi, H. Lin, W. Li, X. Zhang and Q. Zhang, *Environ. Sci. Pollut. Res.*, 2018, **25**, 32373–32380.
- 70 A. D'Alessandro, A. G. Kriebardis, S. Rinalducci, M. H. Antonelou, K. C. Hansen, I. S. Papassideri and L. Zolla, *Transfusion*, 2015, **55**, 205–219.
- 71 F. Ruggeri, C. Marcott, S. Dinarelli, G. Longo, M. Girasole, G. Dietler and T. Knowles, *Int. J. Mater. Sci.*, 2018, **19**, 2582.
- 72 S. Li, Z. Chi and W. Li, *Environ. Pollut.*, 2019, **253**, 239–245.
- 73 W. Fang, Z. Chi, W. Li, X. Zhang and Q. Zhang, *J. Nanobiotechnol.*, 2019, **17**, 66.
- 74 K. Sahoo, R. S. H. Koralege, N. Flynn, S. Koteeswaran, P. Clark, S. Hartson, J. Liu, J. D. Ramsey, C. Pope and A. Ranjan, *Pharm. Res.*, 2016, **33**, 1191–1203.
- 75 S.-Q. Li, R.-R. Zhu, H. Zhu, M. Xue, X.-Y. Sun, S.-D. Yao and S.-L. Wang, *Food Chem. Toxicol.*, 2008, **46**, 3626–3631.
- 76 Y. Heo, C.-A. Li, D. Kim and S. Shin, *Clin. Hemorheol. Microcirc.*, 2017, **65**, 49–56.
- 77 J. Kim, M. Nafiujjaman, M. Nurunnabi, Y.-K. Lee and H.-K. Park, *Food Chem. Toxicol.*, 2016, **97**, 346–353.
- 78 J. Kim, Y.-J. Heo and S. Shin, *Clin. Hemorheol. Microcirc.*, 2016, **62**, 99–107.
- 79 H. Steuer, R. Krastev and N. Lemberg, *J. Biomed. Mater. Res.*, 2014, **102**, 897–902.
- 80 P. V. Asharani, S. Sethu, S. Vadukumpully, S. Zhong, C. T. Lim, M. P. Hande and S. Valiyaveetil, *Adv. Funct. Mater.*, 2010, **20**, 1233–1242.
- 81 J. H. Lee, M. Gulumian, E. M. Faustman, T. Workman, K. Jeon and I. J. Yu, *BioMed Res. Int.*, 2018, **2018**, 1–10.
- 82 M. Sopjani, M. Föller and J. Haendeler, *J. Appl. Toxicol.*, 2009, **29**, 531–536.
- 83 A. Nemmar, S. Beegam, P. Yuvaraju, J. Yasin, A. Shahin and B. H. Ali, *Cell. Physiol. Biochem.*, 2014, **34**, 255–265.
- 84 T. Yu, A. Malugin and H. Ghandehari, *ACS Nano*, 2011, **5**, 5717–5728.
- 85 I. I. Slowing, C.-W. Wu, J. L. Vivero-Escoto and V. S.-Y. Lin, *Small*, 2009, **5**, 57–62.

